Toxicology and Applied Pharmacology 278 (2014) 1–8

Contents lists available at ScienceDirect

Toxicology and Applied Pharmacology

journal homepage: www.elsevier.com/locate/ytaap

Exploring the potential role of tungsten carbide cobalt (WC-Co) nanoparticle internalization in observed toxicity toward lung epithelial cells *in vitro* ☆

Andrea L. Armstead [a,b], Christopher B. Arena [a,c], Bingyun Li [a,b,c,d,*]

[a] Biomaterials, Bioengineering & Nanotechnology Laboratory, Department of Orthopaedics, School of Medicine, West Virginia University, Morgantown, WV 26506, USA
[b] Pharmaceutical and Pharmacological Sciences Graduate Program, School of Pharmacy, West Virginia University, Morgantown, WV 26506, USA
[c] E.J. Van Liere Research Program, School of Medicine, West Virginia University, Morgantown, WV 26506, USA
[d] Mary Babb Randolph Cancer Center, Morgantown, WV 26506, USA

ARTICLE INFO

Article history:
Received 7 November 2013
Revised 31 March 2014
Accepted 6 April 2014
Available online 16 April 2014

Keywords:
Nanotoxicity
Nanoparticle
Hard metal
Lung disease
Pulmonary exposure
Internalization

ABSTRACT

Tungsten carbide cobalt (WC-Co) has been recognized as a workplace inhalation hazard in the manufacturing, mining and drilling industries by the National Institute of Occupational Safety and Health. Exposure to WC-Co is known to cause "hard metal lung disease" but the relationship between exposure, toxicity and development of disease remain poorly understood. To better understand this relationship, the present study examined the role of WC-Co particle size and internalization on toxicity using lung epithelial cells. We demonstrated that nano- and micro-WC-Co particles exerted toxicity in a dose- and time-dependent manner and that nano-WC-Co particles caused significantly greater toxicity at lower concentrations and shorter exposure times compared to micro-WC-Co particles. WC-Co particles in the nano-size range (not micron-sized) were internalized by lung epithelial cells, which suggested that internalization may play a key role in the enhanced toxicity of nano-WC-Co particles over micro-WC-Co particles. Further exploration of the internalization process indicated that there may be multiple mechanisms involved in WC-Co internalization such as actin and microtubule based cytoskeletal rearrangements. These findings support our hypothesis that WC-Co particle internalization contributes to cellular toxicity and suggest that therapeutic treatments inhibiting particle internalization may serve as prophylactic approaches for those at risk of WC-Co particle exposure.

© 2014 Elsevier Inc. All rights reserved.

Introduction

The effects of nanomaterial inhalation and pulmonary exposure are intense areas of research, as this is one of the most common routes by which humans are exposed to nanomaterials or nanoparticles in their environments (Nurkiewicz et al., 2011; Simeonova and Erdely, 2009). Although the effects of exposure vary due to the material and composition of the particles, pulmonary effects of nanoparticle exposure are known to include lung toxicity, inflammation, asthma, pleural effusion, pulmonary fibrosis, granuloma formation, etc (Li et al., 2010; Song et al., 2009). Inhalation of nanoparticles is a concern not only for the casual consumer, but also as an occupational hazard for industry workers whose daily tasks include the manufacture, production or repeated use of nanoparticle-containing goods, tools and equipment.

In particular, occupational exposure to tungsten carbide cobalt (WC-Co), a hard composite metal commonly used as a material or coating for tools and machinery in mining and drilling industries (Yao et al., 1998) is a concern. Exposure typically occurs via inhalation in the workplace, as WC-Co "dusts" are released into the air upon extensive and repeated use of these tools, such as drills, in a closed environment. Inhalation of WC-Co "dusts", composed of various-sized WC-Co particles, is well-documented to cause occupational asthma, hard metal lung disease (HMLD) and an increased (e.g. two-fold) risk for lung cancer (Balmes, 1987; Chiappino, 1994; Cugell, 1992; Day et al., 2009; Kraus et al., 2001; Lasfargues et al., 1994; Migliori et al., 1994; Moriyama et al., 2007; Moulin et al., 1998; Naqvi et al., 2008; Nemery and Abraham, 2007; Yao et al., 1998). Among pulmonary diseases, HMLD is difficult to diagnose as its symptoms are similar to other respiratory ailments. HMLD usually manifests as progressive inflammation and fibrosis of the lung, with some cases progressing to lung cancer (Moriyama et al., 2007; Naqvi et al., 2008; Nemery and Abraham, 2007; Nemery et al., 2001; Rivolta et al., 1994; Ruokonen et al., 1996). At present, the

☆ On average, our publications have been cited 3.2 times/paper/year (h-index = 21; http://www.hsc.wvu.edu/som/ortho/bli/resume/publications.aspx).

* Corresponding author at: Biomaterials, Bioengineering & Nanotechnology Laboratory, Department of Orthopaedics, School of Medicine, West Virginia University, 1 Medical Center Drive, Morgantown, WV 26506-9196, USA. Fax: +1 304 293 7070.
E-mail address: bili@hsc.wvu.edu (B. Li).
URL: http://www.hsc.wvu.edu/som/ortho/bli/ (B. Li).

http://dx.doi.org/10.1016/j.taap.2014.04.008
0041-008X/© 2014 Elsevier Inc. All rights reserved.

relationship between WC-Co exposure, toxicity and development of HMLD remains poorly understood.

Since the first recognition of adverse health effects from WC-Co exposure in the 1960s (Bech et al., 1962; Beritic et al., 1963; Heuer, 1962; Joseph, 1968; Trautmann, 1958), there have been a number of reports regarding the toxicity of WC-Co in the literature both *in vitro* (Anard et al., 1997; Antonini et al., 2000; Bastian et al., 2009; Busch et al., 2010; De Boeck et al., 2003b; Ding et al., 2009; Edel et al., 1990; Fedan and Cutler, 2001; Kuhnel et al., 2009; Lison and Lauwerys, 1990, 1992, 1993; Lison et al., 1995; Lombaert et al., 2008, 2012; Roesems et al., 2000; Zhang et al., 2010) and *in vivo* (Adamis et al., 1997; De Boeck et al., 2003a; Huaux et al., 1995; Kerfoot et al., 1975; Kitamura et al., 1980; Lasfargues et al., 1992, 1995; Rengasamy et al., 1999). While it is well established that composite WC-Co particles are more toxic than tungsten (W), tungsten carbide (WC) or cobalt (Co) alone, the potential contribution of WC-Co particle internalization toward observed toxicity and the mechanism by which WC-Co particles could be internalized by relevant cells has not been well-addressed. The present study examined the toxic effects and explored potential internalization mechanism(s) of nano- and micro-sized WC-Co particles in lung epithelial cells.

Materials and methods

Materials and Reagents

Micro-sized WC-Co particles (micro-WC-Co; 4 μm) were purchased from Alfa Aesar (Ward Hill, MA) and nano-sized WC-Co particles (nano-WC-Co; 80 nm) were purchased from Inframat Advanced Materials (Manchester, CT). BEAS-2B lung epithelial cells were obtained from the laboratory of Yon Rojansakul. Dulbecco's Modified Eagle Media (DMEM), sterile phosphate buffered saline (PBS), 0.25% trypsin/ethylenediaminetetraacetic acid (EDTA), fetal bovine serum (FBS) and penicillin/streptomycin were purchased from Lonza (Allendale, NJ). The MTT cell viability kit (TOX-1), 2′,7′-dichlorofluorescein diacetate (DCF), dihydroethidium (DHE), monodansylcadaverine (MDC), colchicine and cytochalasin-D, glutaraldehyde, paraformaldehyde, agarose and osmium tetroxide were purchased from Sigma-Aldrich (St. Louis, MO). ApoScreen flow cytometry kit, including annexin-V-FITC (AV-FITC) and propidium iodide (PI), was purchased from Southern Biotech Inc. (Birmingham, AL). SPI-PON 812 for electron microscopy was purchased from SPI Supplies (West Chester, PA).

Particle preparation

For cell culture experiments, stock WC-Co particle suspensions (5 mg/mL) were prepared in sterile PBS containing 10% FBS and sonicated using an Omni International Sonic Ruptor 250 Ultrasonic Homogenizer (Kennesaw, GA). Stock particle suspensions were sonicated under 120 watts power output, at a frequency of 20 kHz, in two 30-second intervals to ensure particle dispersion. Sonication was performed in 30 mL plastic vials immobilized in an ice bath to minimize heating of the suspension during the sonication process. Dilute particle suspensions (0.1 to 1000 μg/mL) were prepared in DMEM containing 10% FBS from the 5 mg/mL stock particle suspension on the day of each experiment.

Particle characterization

Micro- and nano-WC-Co particles were characterized after preparation in suspension for cell culture, described above, via dynamic light scattering (DLS, Malvern Zetasizer version 7.01, Malvern Instruments Ltd, Malvern, UK), transmission electron microscopy (TEM; Zeiss Libra 120 electron microscope, Carl Zeiss Microscopy, Jena, Germany), scanning electron microscopy and energy-dispersive x-ray for the determination of elemental composition (SEM/EDX; JEOL JSM 7600 F, Jeol USA, Inc, Peabody, MA). Further detail provided in ***Supplementary Material.***

Cell culture and exposure to WC-Co particles

BEAS-2B cells were cultured in DMEM supplemented with 10% FBS and 1% penicillin-streptomycin and maintained at 37 °C and 5% CO_2. Briefly, confluent monolayers were rinsed with PBS, trypsinized, transferred to 5 mL polystyrene tubes and centrifuged at 1200 rpm for 7 min to pellet. The cell pellet was re-suspended at the desired plating density, transferred to a tissue culture plate and allowed to adhere overnight. Ninety-six well plates were seeded at 1.5×10^5 cells/mL for viability, oxidative stress and inhibitor assays; 24 well plates were seeded at 2×10^5 cells/mL for apoptosis and TEM examination of particle internalization.

Cell Viability Assay

For the viability assay, cells were exposed to either nano- or micro-WC-Co particles at concentrations of 0.1, 1, 10, 100 and 1000 μg/mL for exposure periods of 0.5, 1, 2, 6, 12 and 48 h. Following particle treatment, cells were rinsed once with sterile PBS to remove traces of media and excess particles. The MTT cell viability assay was performed per kit instructions (TOX-1, Sigma-Aldrich) in a 96 well cell culture plate.The absorbance of each well was recorded at 570 nm using a Bio-Tek μQuant microplate reader (Winooski, VT). Blank values were subtracted from absorbance readings. Cell viability was calculated by dividing the absorbance of particle treated cells (Abs_{Exptl}) by the absorbance of the negative control cells (media treatment only; $Abs_{Control}$) and converted to percentage according to the following equation: Cell Viability (%) = $(Abs_{Exptl} / Abs_{Control}) \times 100\%$.

Oxidative stress assay

Oxidative stress was examined at select nano- and micro-WC-Co particle concentrations of 0.1, 10 and 1000 μg/mL after exposure periods of 0.5, 1, 2, 6, 12 and 48 h. Following particle treatment, cells were rinsed once with sterile PBS to remove traces of media and excess particles. Oxidative stress was then determined by the addition of 10 μM DCF or DHE in PBS following particle treatment. Plates were incubated for 15 min in the dark and then fluorescence intensity of each well was quantified at 520 nm for DCF or 620 nm for DHE. The relative fluorescence of particle-treated cells was calculated as fold over control.

Annexin-V apoptosis assay

Cells were treated with WC-Co particles at select concentrations of 10, 100 and 1000 μg/mL for 12 h. Positive control (apoptotic) cells were prepared by heat-shock for 5 min at 56 °C to induce apoptosis. Following particle exposure/heat treatment, cells were rinsed once with PBS, trypsinized, transferred to 5 mL polystyrene tubes and centrifuged at 1200 rpm for 7 min to pellet. Cell pellets were re-suspended and rinsed twice with 1 mL of PBS to remove traces of media that may interfere with staining. After rinsing, cells were re-suspended in ice-cold binding buffer and stained with AV-FITC and PI according to manufacturer instructions. Samples were analyzed immediately by flow cytometry using a BD FACSCalibur flow cytometer (Franklin Lakes, NJ).

Particle internalization and inhibition assay

Three cytoskeletal inhibitors, each affecting a specific pathway, were studied to explore the potential mechanism(s) by which WC-Co particles could be internalized: 1) MDC; an inhibitor of clathrin-coated pit endocytosis (Schutze et al., 1999), 2) colchicine; an inhibitor of microtubule polymerization (Nunez et al., 1979) and 3) cytochalasin-D; an inhibitor of actin filament polymerization (Cooper, 1987). WC-Co

particle suspensions were prepared as described above with the addition of 10 μg/mL MDC, colchicine or cytochalasin-D. Cell viability was calculated as described above; in this case, control cells received inhibitor treatment only (media + 10 μg/mL inhibitor) such that any background toxicity of the inhibitor itself was accounted for in the resulting cell viability calculation.

Transmission Electron Microscopy (TEM)

Following 12 h, 100 μg/mL WC-Co particle exposure, cells were washed once with PBS, detached using trypsin/EDTA and collected by centrifugation at 1200 rpm. Cell pellets were washed twice with PBS and fixed with 2% para-formaldehyde and 2.5% glutaraldehyde in PBS for 0.5 h at room temperature. Fixed cell samples were transferred to the West Virginia University Tissue Processing & Imaging Core Facility for additional processing. Briefly, fixed cell pellets were washed 3 times with PBS, re-suspended in warm 2% low-melting point agarose solution and centrifuged at 2000 ×g for 5 min. The resulting gelled pellet was post-fixed in a 1% osmium tetroxide for 2 h at room temperature. Post-fixation, the cell pellet was washed 3 times with PBS and dehydrated in a graded ethanol series followed by propylene oxide. Next, the cells were embedded in SPI-PON 812 solution and polymerized at 60 °C for 48 h. Thin sections (50 nm) were cut and mounted on copper grids and subsequently imaged using a Zeiss Libra 120 electron microscope at 120 kV (Carl Zeiss Microscopy, Jena, Germany). A minimum of 200 cells were examined for the presence of WC-Co particles per mounted sample, with at least 20 sample grids examined per treatment group. The presence of tungsten (W) in cells showing internalized WC-Co particles was confirmed using electron energy loss spectroscopy (EELS; see Supplementary Material).

Statistical Analyses

All experiments were performed in triplicate and data are presented as mean ± standard deviation. Statistical analysis was carried out by 2-way analysis of variance (ANOVA) using GraphPad Prism software (La Jolla, CA). P values < 0.05 were considered significant.

Results

WC-Co particle characterization

Dynamic light scattering analysis of WC-Co particles in suspension revealed a narrow nano-WC-Co particle size distribution, with a calculated average particle size of 98 nm verified by TEM imaging (Figs. 1A and C). For the micro-WC-Co particles, size distribution was slightly larger with a calculated average particle size of 3.4 μm, also confirmed by TEM imaging (Figs. 1B and D). EDX analysis of raw WC-Co powder showed that nano-WC-Co contained oxygen in addition to tungsten and cobalt (Table 1 and Figs. S1, S2).

WC-Co effects on cell viability and oxidative stress

Lung epithelial BEAS-2B cells were exposed to WC-Co particles at concentrations of 0.1, 1, 10, 100 and 1000 μg/mL for durations of 0.5, 1, 2, 6, 12 and 48 h. In cells exposed to nano-WC-Co particles (Fig. 2A), a significant reduction in viability (compared to control) was observed at concentrations of 10, 100 and 1000 μg/mL for all the exposure time periods studied. Significant reduction in viability was also observed at concentrations of 0.1 and 1 μg/mL after 48 h of exposure. In cells exposed to micro-WC-Co (Fig. 2B), significant reduction in viability

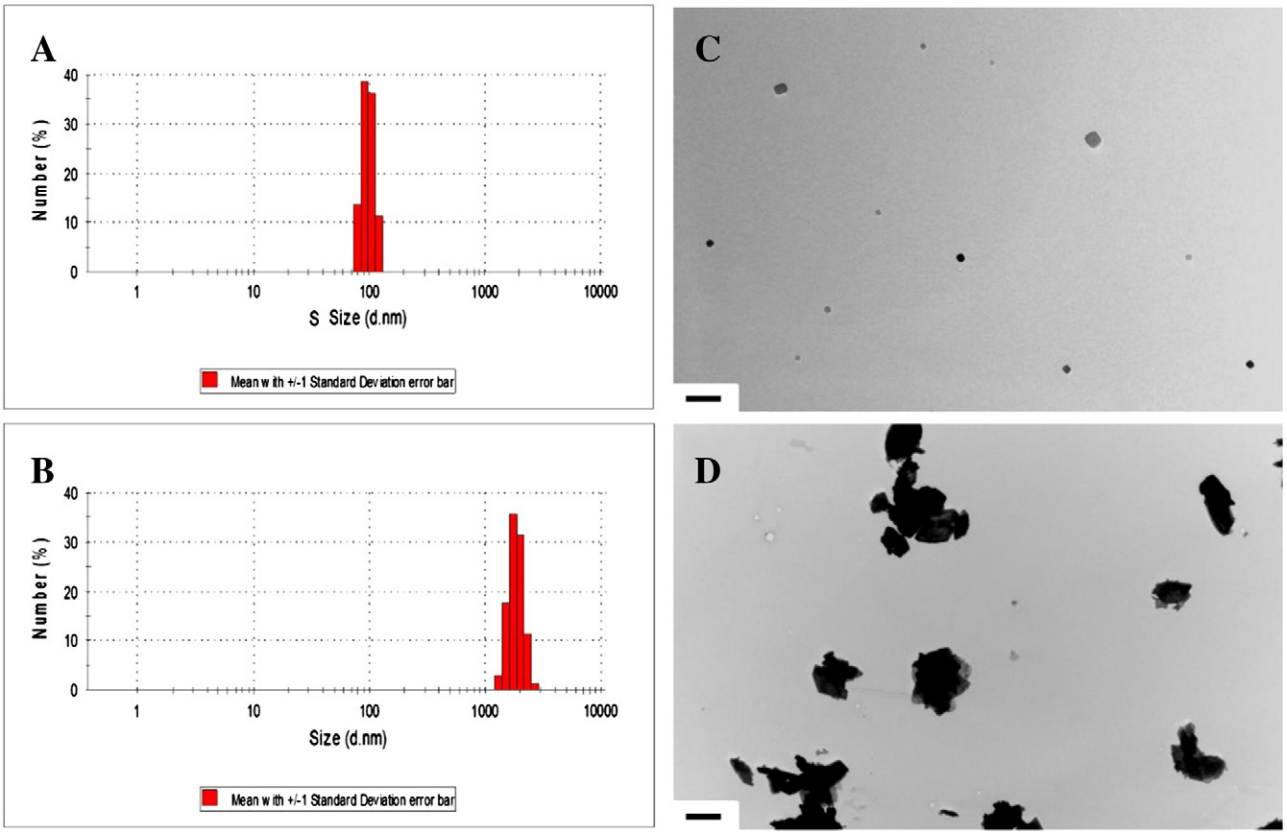

Fig. 1. WC-Co particle characterization via dynamic light scattering (DLS) of A) nano-WC-Co and B) micro-WC-Co particles suspended in cell culture media (average size = 98 nm and 3.4 μm, respectively) and representative TEM images of C) nano-WC-Co (scale bar = 500 nm) and D) micro-WC-Co (scale bar = 2 μm) particles.

Table 1
Elemental composition of nano- and micro-WC-Co particles by weight percentage determined using energy-dispersive X-ray (EDX).

Particle sample	Tungsten (W)	Cobalt (Co)	Carbon (C)	Oxygen (O)
Nano-WC-Co (avg. size 98 nm)	72.13	13.42	7.63	6.81
Micro-WC-Co (avg. size 3.4 μm)	86.53	5.06	8.40	0.00

(compared to control) was observed at concentrations of 100 and 1000 μg/mL at 2, 6, 12 and 48 h of exposure. Significant reduction in viability was also observed at 1 and 10 μg/mL after 48 h of exposure. Moreover, nano-WC-Co particle exposure resulted in significantly higher reduction in cell viability overall compared to micro-WC-Co particles (Fig. S3). For instance, the cell viability following nano-WC-Co exposure was significantly lower than the viability following micro-WC-Co exposure (Fig. S3) at 1000 μg/mL for all exposure periods studied except at 48 h, where the cell viability for both particle exposures was very low (Fig. S3F). Significantly lower cell viability was also observed in nano-WC-Co compared to micro-WC-Co particle exposure at 0.5 h from 10 to 1000 μg/mL (Fig. S3A).

Oxidative stress was measured in the form of DCF/DHE fluorescence after exposure to WC-Co particles at 0.1, 10, 1000 μg/mL at representative low, moderate and highly toxic particle concentrations determined in Figs. 2A, B. Compared to control, there was a significant increase in DCF fluorescence in cells exposed to 1000 μg/mL nano- and micro-WC-Co particles over the exposure periods studied (0.5, 1, 2, 6, 12, and 48 h) and no significant difference when exposed to 0.1 and 10 μg/mL (Figs. 2C and S4A). Maximal DCF fluorescence was observed for 1000 μg/mL nano- and micro-WC-Co after 1 h of exposure, where DCF fluorescence due to nano-WC-Co exposure was significantly higher than micro-WC-Co (Fig. 2C). Compared to control, there were no significant differences in DHE fluorescence observed for cells exposed to nano- or micro-WC-Co at any concentration or exposure period tested (Fig. S4B).

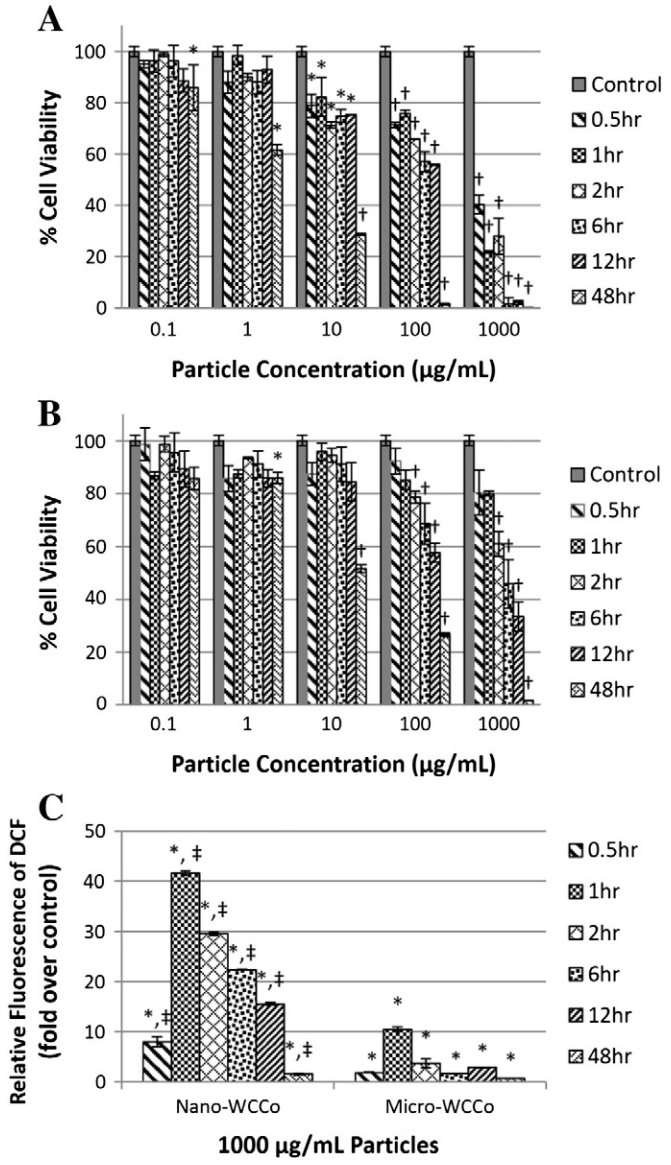

Fig. 2. Cell viability after A) nano-WC-Co and B) micro-WC-Co particle exposure and C) oxidative stress indicated by DCF fluorescence after exposure to 1000 μg/mL nano- and micro-WC-Co particles. (*P < 0.05, †P < 0.001 compared to control, ‡P < 0.05 compared to micro-WC-Co).

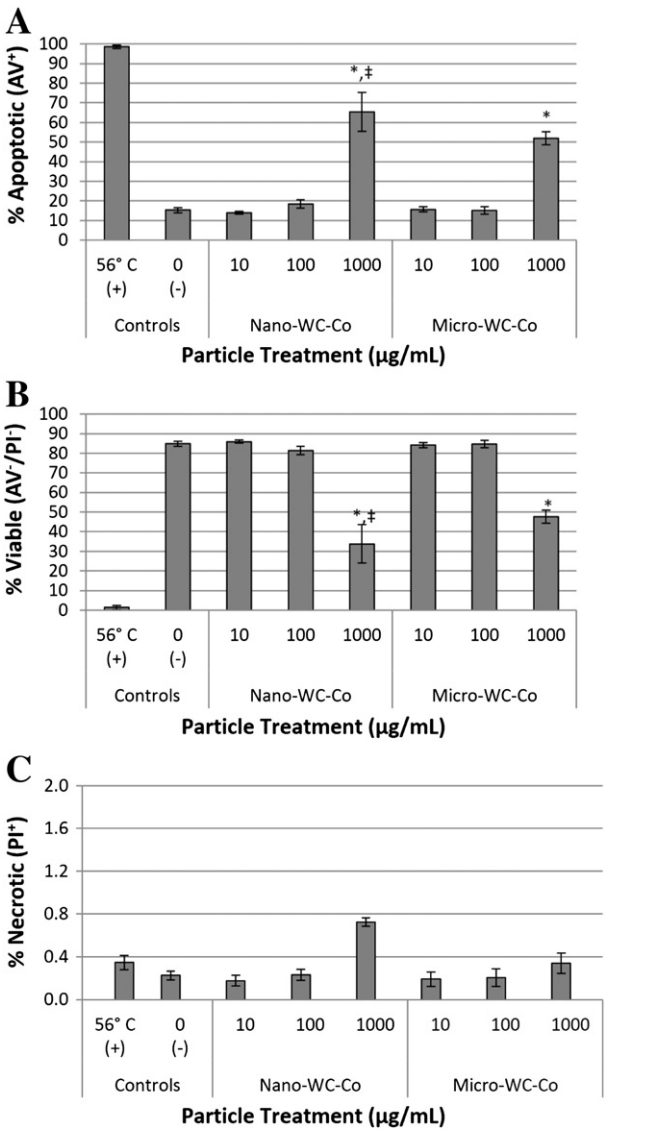

Fig. 3. Summary of flow cytometry staining profiles after 12 h WC-Co particle exposure: A) total percentage of apoptotic cells (AV^+/PI^+ and AV^+/PI^-; sum total of upper and lower right quadrants), B) total percentage of viable cells (AV^-/PI^-; lower left quadrant) and C) total percentage of necrotic cells (PI^+/AV^-; upper left quadrant) (*P < 0.05 compared to control, ‡P < 0.05 compared to micro-WC-Co).

Induction of apoptosis in WC-Co exposed cells

The total percentage of apoptotic, necrotic or viable BEAS-2B cells determined by flow cytometry after exposure to WC-Co is shown in Fig. 3. Cells stimulated to undergo apoptosis by heat treatments at 56 °C were included as a positive control for reference. A dose-dependent increase in the total percentage of apoptotic cells was observed with increasing WC-Co particle concentration for nano- and micro-WC-Co particles (Fig. 3A). Compared to negative control, a significantly higher percentage of apoptotic cells was observed at 1000 μg/mL for both nano- and micro-WC-Co particles (Fig. 3A). A corresponding dose-dependent decrease in the percentage of viable cells was also observed and a significantly lower percentage of viable cells, compared to control, was found at 1000 μg/mL for both nano- and micro-WC-Co particles (Fig. 3B). The percentage of necrotic cells remained low, less than 1% for cells exposed to nano- and micro-WC-Co (Fig. 3C). A significant difference in the percentage of apoptotic cells was observed at the highest particle concentration of 1000 μg/mL, where nano-WC-Co treatment showed significantly higher apoptosis than micro-WC-Co treatment (Fig. 3A) and the percentage of viable cells after nano-WC-Co treatment was significantly lower than micro-WC-Co treatment (Fig. 3B).

Particle internalization and inhibition

After 6 h of nano-WC-Co exposure, there was a significant increase in cell viability compared to control (cells receiving particle treatment only, no inhibitor) in the presence of MDC, colchicine and cytochalasin D at WC-Co concentrations of 10, 100 and 1000 μg/mL (Fig. 4A). After 12 h, significant increases in cell viability were observed in the presence MDC and colchicine at 100 μg/mL nano-WC-Co and in the presence of cytochalasin D at 10, 100 and 1000 μg/mL nano-WC-Co (Fig. 4B). After 48 h, significant increases in cell viability were observed for MDC and colchicine at 10 and 100 μg/mL whereas cytochalasin D caused a significant increase in viability for 10, 100 and 1000 μg/mL nano-WC-Co (Fig. 4C).

For cells exposed to micro-WC-Co particles, a significant increase in cell viability was observed after 6 and 12 h in the presence of MDC and colchicine at 100 μg/mL WC-Co (Figs. 4A and B). In the presence of cytochalasin D, significant increases in cell viability were observed after 6 h for 100 and 1000 μg/mL WC-Co and after 12 h at 10, 100 and 1000 μg/mL micro-WC-Co (Figs. 4A and B). After 48 h, significant increases in cell viability were observed for MDC and colchicine at 10 and 100 μg/mL and in the presence of cytochalasin D at 10, 100 and 1000 μg/mL micro-WC-Co (Fig. 4C).

Compared to micro-WC-Co exposure, nano-WC-Co particle exposure led to significantly lower cell viability after 6 h in the presence of MDC and cytochalasin D at 100 and 1000 μg/mL and in the presence of colchicine at 1000 μg/mL (Figs. S6A, S7A, S8A). After 12 h of exposure, nano-WC-Co particles resulted in significantly lower cell viability than micro-WC-Co particles in the presence of all 3 inhibitors at particle concentration of 1000 μg/mL (Figs. S6B, S7B, S8B). After 48 h, the cell viability after nano-WC-Co exposure was significantly lower than that of micro-WC-Co exposure in the presence of MDC at 10 and 100 μg/mL, colchicine at 10 μg/mL and cytochalasin D at 1000 μg/mL (Figs. S6C, S7C, S8C).

Representative TEM images of BEAS-2B cells exposed to 100 μg/mL WC-Co particles for 12 h are shown in Fig. 5. We found that nano-WC-Co particles had been internalized (visible as distinct black dots, denoted by arrows) and were localized in the cytoplasm within the outer cell membrane (Fig. 5B). For cells exposed to micro-WC-Co, no particles of micron size were detected within the cells; however, several particles with diameter of approximately 500 nm were found localized in the cytoplasm (Fig. 5C). In the presence of cytochalasin D, no particles were found within the cytoplasm of nano-WC-Co exposed cells (Fig. 5D). The presence of tungsten in representative particle-treated cells (Fig. 5) was confirmed using EELS, where a definite tungsten peak was identified at ~ 1850 eV (Fig. S9) which confirmed the presence of WC-Co particles within the cytoplasm shown in Fig. 5.

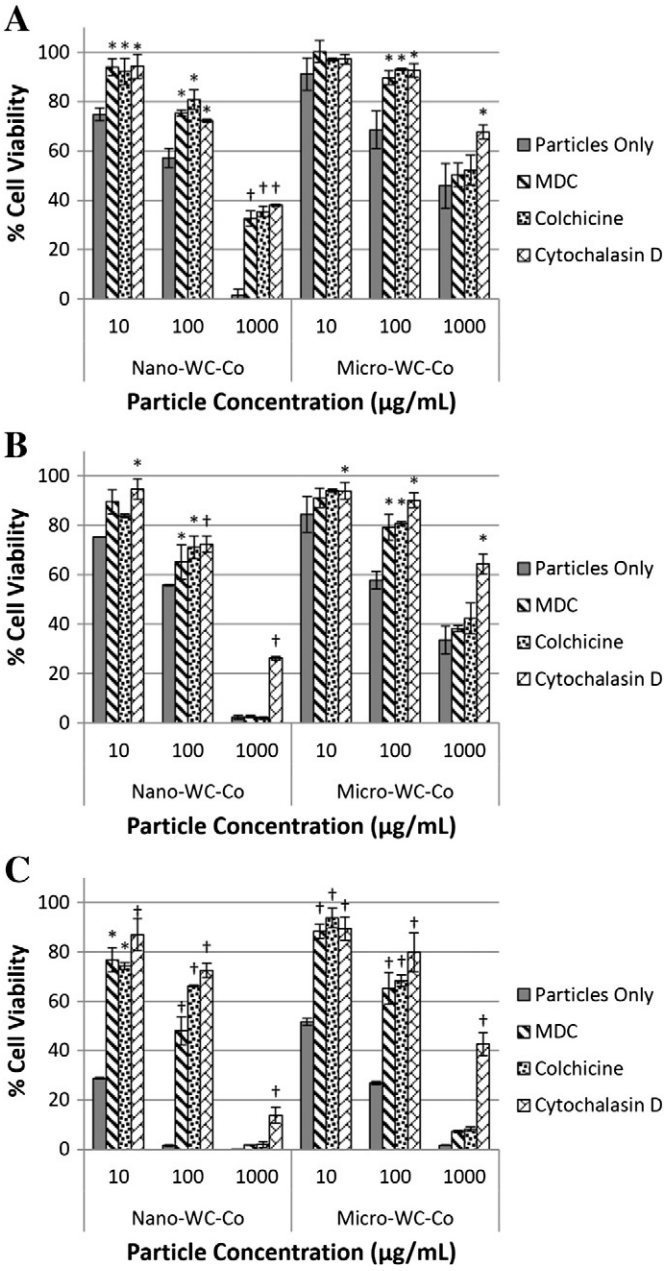

Fig. 4. Cell viability after exposure to nano- or micro-WC-Co particles in the presence of 10 μg/mL cytoskeletal inhibitors MDC, colchicine or cytochalasin D after A) 6 h, B) 12 h and C) 48 h. [*P < 0.05, †P < 0.001 compared to control (particles only)].

Discussion

While workplace exposure limits are defined for hard metal manufacturing facilities (Kraus et al., 2001; Stefaniak et al., 2007, 2009), it is difficult to predict the resulting lung burden of inhaled WC-Co per person (Naqvi et al., 2008) and challenging to define a relevant dosing scheme for experimental studies. Since exposure limits are frequently defined on a mass-per-volume basis (i.e. mg per m^3), we elected to deliver our nano- and micro-WC-Co particles at equivalent mass-per-volume doses and intentionally encompassed a large concentration range, 0.1 to 1000 μg/mL, to cover the range in total lung particle mass burden that would be observed in workers exposed through

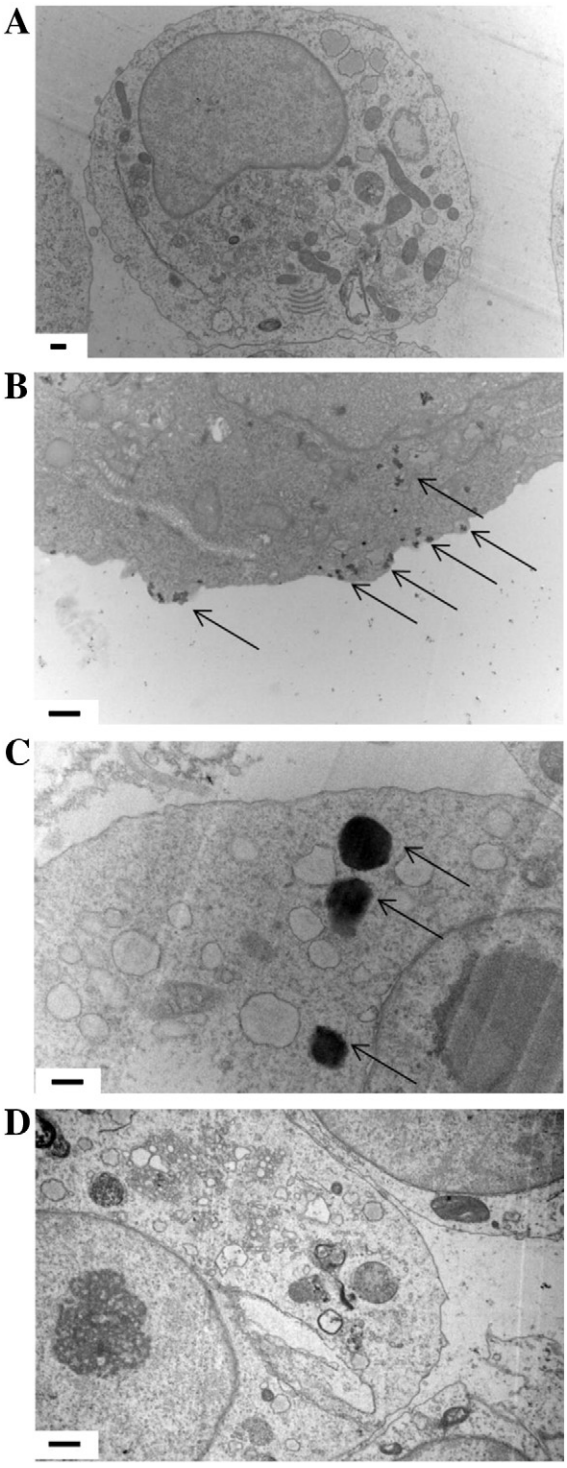

Fig. 5. Representative TEM images of A) non-exposed control cells, B) cells exposed to 100 μg/mL nano-WC-Co for 12 h, C) cells exposed to 100 μg/mL micro-WC-Co for 12 h and D) cells exposed to 100 μg/mL nano-WC-Co plus 10 μg/mL cytochalasin D for 12 h. Arrows denote WC-Co particles; scale bars = 0.5 μm.

occupational settings. As shown in Fig. 2, nano-WC-Co was significantly more toxic than micro-WC-Co at concentrations ≥ 10 μg/mL. These data are consistent with our expectations and similar to toxicity reported in the literature (Anard et al., 1997; Bastian et al., 2009; Busch et al., 2010; De Boeck et al., 2003a, 2003b; Kuhnel et al., 2009, 2012; Lombaert et al., 2004, 2008, 2012). Since reasonable measures were taken to address the potential artifacts (Figs. S10–16) due to particle interference with our *in vitro* assays (Guadagnini et al., 2013; Holder et al., 2012; Kroll et al., 2012; Val et al., 2009; Wilhelmi et al., 2012), the differences in our observed toxicity were probably due to the smaller size, higher resulting particle number and increased surface area of the nano-WC-Co compared to the micro-WC-Co particles. These factors are known to play a critical role in particle toxicity and uptake regardless of material composition (Canton and Battaglia, 2012; Champion and Mitragotri, 2006; dos Santos et al., 2011; Wu et al., 2012; Zhang and Monteiro-Riviere, 2009; Zhao and Castranova, 2011).

The role of apoptosis in hard metal lung disease remains unclear; however, earlier studies have demonstrated the apoptogenic potential of WC-Co particles *in vitro* (Lombaert et al., 2004). Since there are known roles for the regulation/dysregulation of apoptotic processes in cancer progression (Holdenrieder and Stieber, 2010; Shivapurkar et al., 2003; Stieber and Holdenrieder, 2010) and it is reported that HMLD patients are at a two-fold increased risk of developing lung cancer (Lasfargues et al., 1994; Moulin et al., 1998), it seemed appropriate to examine the effects of WC-Co exposure on the induction of apoptosis in our lung epithelial cell model (Stearns et al., 2001). We confirmed that WC-Co exposure induces apoptosis in exposed cell populations after 12 h in the present study (Figs. 3, S5). We believe in the possibility that WC-Co induced apoptosis may play a role in HMLD progression and contribute to the increased risk of lung cancer; however, the exact mechanism and contribution of these factors remains to be elucidated.

Interestingly, our apoptosis findings (Fig. 3) did not correlate directly with our viability data shown in Fig. 2; greater toxicity was determined in the MTT viability assay than was observed by quantification of annexin-V-positive (apoptotic/dead) cells in our flow cytometry assay. We attributed the variance in observed WC-Co toxicity to the differences in assay methodology and approach: while the MTT assay relies on the conversion of the tetrazolinium substrate to formazan by live cells, the annexin-V flow cytometry assay relies on membrane surface staining of exposed phosphatidyl serine (PS) residues, a known marker for apoptotic cells. In this case, we believe that after WC-Co treatment, some of the cells may have reduced metabolic function but are not yet undergoing apoptosis, which would be reflected in the MTT assay as a reduction in viability; however, these same cells would not be quantified as apoptotic (dead) by the AV-FITC apoptosis assay since they may not yet have externalized PS residues available for staining. However, our data confirmed that WC-Co is capable of inducing apoptosis. Additionally, our data regarding the limited capacity of WC-Co particle exposure to stimulate oxidative stress at low concentrations (<1000 μg/mL, Fig. S4) appears to be consistent with earlier *in vitro* studies in other cells (Kuhnel et al., 2012; Lison and Lauwerys, 1992, 1993; Lison et al., 1995; Zhang et al., 2010). Although oxidative stress has been implicated as the toxic mechanism for other nanomaterials such as silica or titanium dioxide (Park et al., 2008; Sun et al., 2011), our data suggest that oxidative stress is probably not a primary mechanism of WC-Co toxicity.

Hard metal WC-Co particle internalization is of particular interest because hard metal deposits have been found in lung biopsy specimens from patients with hard metal lung disease (Chiappino, 1994; Dunlop et al., 2005; Gotway et al., 2002; Kusaka et al., 1984; Mariano et al., 1994; Matejka et al., 1985; Moriyama et al., 2007; Nemery and Abraham, 2007; Rizzato et al., 1992) which may suggest a potential role for particle internalization and/or deposition in the disease state. Studying how WC-Co particle internalization occurs *in vitro* may offer a better understanding of how these deposits may form *in vivo*, which may allow for the development of improved HMLD treatment strategies or new prophylactic approaches (Armstead and Bingyun, 2011; Luo et al., 2012; Wang et al., 2013) for those at risk of exposure. It has been reported that alveolar epithelial cells are capable of internalizing nanoparticles (Stearns et al., 2001) and we confirmed in this study that WC-Co particles are capable of being internalized (Bastian et al., 2009) in our lung epithelial cell model as shown in Fig. 5. Based on our findings from the cytoskeletal inhibitor assay shown in Fig. 4, we believe that WC-Co particle internalization plays a role in WC-Co mediated

toxicity because a significant increase in cell viability was observed for all three inhibitors tested when compared to cells treated with WC-Co particles only.

The extent of this "rescue" effect varied amongst the inhibitors; however, cytochalasin D appeared to have the most significant effect of the three inhibitors (Fig. 4C), so we hypothesized that actin dynamics and polymerization, inhibited by the presence of cytochalasin D (Cooper, 1987; Goddette and Frieden, 1986), may play a major role in the internalization of WC-Co particles. Additionally, we did not find any internalized WC-Co particles in cells treated with cytochalasin D shown in Fig. 5. A significant increase in cell viability was also observed in the presence of colchicine and MDC, so the potential for multiple mechanisms of internalization cannot be excluded from this study. Colchicine, known to inhibit microtubule polymerization (Elkjaer et al., 1995; Nunez et al., 1979), can interrupt the formation of endocytic vesicles which may also play a role in WC-Co internalization as indicated by the increase in cell viability observed in Fig. 4. However, colchicine was ineffective at reducing WC-Co toxicity at the highest concentration of particles after 48 h (Fig. 4C), so we believe that microtubule-dependent internalization processes are likely secondary to actin-mediated processes affected by cytochalasin D. MDC is an inhibitor of clathrin (Elkjaer et al., 1995; Schutze et al., 1999) and specifically blocks clathrin-mediated endocytosis. In our study, MDC caused the least significant increase in cell viability following WC-Co exposure so we do not believe that clathrin-pit mediated endocytosis is a primary mechanism for WC-Co particle internalization. Taken together, these initial findings suggest a potential role for WC-Co particle internalization in observed toxicity toward lung epithelial cells.

Conclusion

This study examined the toxicity of nano- and micro-sized WC-Co particles and explored the potential role of particle internalization in observed toxicity toward lung epithelial cells. Nano-WC-Co was found to be more toxic than micro-WC-Co as expected and we determined that WC-Co particles are capable of being internalized (via TEM). The presence of cytochalasin D, colchicine and MDC all caused a reduced toxicity, which suggests that there may be multiple mechanisms involved in WC-Co internalization and toxicity. Therefore, internalization of WC-Co particles by cells lining the respiratory tract and lung is possible and may be a potential source of hard metal deposits found in HMLD biopsy specimens.

Conflict of Interest

None.

Acknowledgment

The authors thank Yon Rojanasakul for providing the BEAS-2B cells and Bing-Hua Jiang for WC-Co particle samples. The authors acknowledge the WVU Biochemistry Shared Facilities, the WVU Flow Cytometry Core facility and Kathy Brundage for instrument use and assistance (National Institutes of Health grant #P303M103488, P30RR0321R8). Thanks to Dale Porter for assistance with particle characterization and dynamic light scattering. Special thanks to Dr. Ava Dykes for assistance with electron microscopy experiments performed in the West Virginia University Tissue Processing and Analysis Core Facility, supported in part by National Institutes of Health grant #P30RR031155. The authors thank Suzanne Danley for proofreading.

Declaration of interests

Fellowship funding to A. Armstead was provided by the West Virginia University NANOSAFE graduate fellowship program 2010-12 (formerly WVNano; NSF Cooperative Agreement #1003907) and by the American Foundation for Pharmaceutical Education (Pre-Doctoral Fellowship in Pharmaceutical Science, 2012-14).

Appendix A. Supplementary data

Supplementary data to this article can be found online at http://dx.doi.org/10.1016/j.taap.2014.04.008.

References

Adamis, Z., Tatrai, E., Honma, K., Karpati, J., Ungvary, G., 1997. A study on lung toxicity of respirable hard metal dusts in rats. Ann. Occup. Hyg. 41, 515–526.
Anard, D., Kirsch-Volders, M., Elhajouji, A., Belpaeme, K., Lison, D., 1997. In vitro genotoxic effects of hard metal particles assessed by alkaline single cell gel and elution assays. Carcinogenesis 18, 177–184.
Antonini, J.M., Starks, K., Roberts, J.R., Millecchia, L., Yang, H.M., Rao, K.M., 2000. Changes in F-actin organization induced by hard metal particle exposure in rat pulmonary epithelial cells using laser scanning confocal microscopy. In Vitro Mol. Toxicol. 13, 5–16.
Armstead, A.L., Li, B., 2011. Nanomedicine as an emerging approach against intracellular pathogens. Int. J. Nanomedicine 6, 3281–3293.
Balmes, J.R., 1987. Respiratory effects of hard-metal dust exposure. Occup. Med. 2, 327–344.
Bastian, S., Busch, W., Kuhnel, D., Springer, A., Meissner, T., Holke, R., Scholz, S., Iwe, M., Pompe, W., Gelinsky, M., Potthoff, A., Richter, V., Ikonomidou, C., Schirmer, K., 2009. Toxicity of tungsten carbide and cobalt-doped tungsten carbide nanoparticles in mammalian cells in vitro. Environ. Health Perspect. 117, 530–536.
Bech, A.O., Kipling, M.D., Heather, J.C., 1962. Hard metal disease. Br. J. Ind. Med. 19, 239–252.
Beritic, T., Prpic Majic, D., Mark, B., Markicevic, A., Vurdelja, B., 1963. Pheumoconiosis Caused by Hard Metal Dust. Arh. Hig. Rada Toksikol. 14, 261–268.
Busch, W., Kuhnel, D., Schirmer, K., Scholz, S., 2010. Tungsten carbide cobalt nanoparticles exert hypoxia-like effects on the gene expression level in human keratinocytes. BMC Genomics 11, 65.
Canton, I., Battaglia, G., 2012. Endocytosis at the nanoscale. Chem. Soc. Rev. 41, 2718–2739.
Champion, J.A., Mitragotri, S., 2006. Role of target geometry in phagocytosis. Proc. Natl. Acad. Sci. U. S. A. 103, 4930–4934.
Chiappino, G., 1994. Hard metal disease: clinical aspects. Sci. Total Environ. 150, 65–68.
Cooper, J.A., 1987. Effects of cytochalasin and phalloidin on actin. J. Cell Biol. 105, 1473–1478.
Cugell, D.W., 1992. The hard metal diseases. Clin. Chest Med. 13, 269–279.
Day, G.A., Virji, M.A., Stefaniak, A.B.., 2009. Characterization of exposures among cemented tungsten carbide workers. Part II: Assessment of surface contamination and skin exposures to cobalt, chromium and nickel. J. Expo. Sci. Environ. Epidemiol. 19, 423–434.
De Boeck, M., Hoet, P., Lombaert, N., Nemery, B., Kirsch-Volders, M., Lison, D., 2003a. In vivo genotoxicity of hard metal dust: induction of micronuclei in rat type II epithelial lung cells. Carcinogenesis 24, 1793–1800.
De Boeck, M., Lombaert, N., De Backer, S., Finsy, R., Lison, D., Kirsch-Volders, M., 2003b. In vitro genotoxic effects of different combinations of cobalt and metallic carbide particles. Mutagenesis 18, 177–186.
Ding, M., Kisin, E.R., Zhao, J., Bowman, L., Lu, Y., Jiang, B., Leonard, S., Vallyathan, V., Castranova, V., Murray, A.R., Fadeel, B., Shvedova, A.A., 2009. Size-dependent effects of tungsten carbide-cobalt particles on oxygen radical production and activation of cell signaling pathways in murine epidermal cells. Toxicol. Appl. Pharmacol. 241, 260–268.
dos Santos, T., Varela, J., Lynch, I., Salvati, A., Dawson, K.A., 2011. Effects of transport inhibitors on the cellular uptake of carboxylated polystyrene nanoparticles in different cell lines. PLoS One 6, e24438.
Dunlop, P., Muller, N.L., Wilson, J., Flint, J., Churg, A., 2005. Hard metal lung disease: high resolution CT and histologic correlation of the initial findings and demonstration of interval improvement. J. Thorac. Imaging 20, 301–304.
Edel, J., Sabbioni, E., Pietra, R., Rossi, A., Torre, M., Rizzato, G., Fraioli, P., 1990. Trace metal lung disease: in vitro interaction of hard metals with human lung and plasma components. Sci. Total Environ. 95, 107–117.
Elkjaer, M.L., Birn, H., Agre, P., Christensen, E.I., Nielsen, S., 1995. Effects of microtubule disruption on endocytosis, membrane recycling and polarized distribution of Aquaporin-1 and gp330 in proximal tubule cells. Eur. J. Cell Biol. 67, 57–72.
Fedan, J.S., Cutler, D., 2001. Hard metal-induced disease: effects of metal cations in vitro on guinea pig isolated airways. Toxicol. Appl. Pharmacol. 174, 199–206.
Goddette, D.W., Frieden, C., 1986. Actin polymerization. The mechanism of action of cytochalasin D. J. Biol. Chem. 261, 15974–15980.
Gotway, M.B., Golden, J.A., Warnock, M., Koth, L.L., Webb, R., Reddy, G.P., Balmes, J.R., 2002. Hard metal interstitial lung disease: high-resolution computed tomography appearance. J. Thorac. Imaging 17, 314–318.
Guadagnini, R., Halamoda Kenzaoui, B., Cartwright, L., Pojana, G., Magdolenova, Z., Bilanicova, D., Saunders, M., Juillerat, L., Marcomini, A., Huk, A., Dusinska, M., Fjellsbo, L.M., Marano, F., Boland, S., 2013. Toxicity screenings of nanomaterials: challenges due to interference with assay processes and components of classic in vitro tests. Nanotoxicology. http://dx.doi.org/10.3109/17435390.2013.829590 (Epub ahead of print, July 27, 2013).
Heuer, W., 1962. Pulmonary fibrosis in hard metal-production workers. Int. Arch. Gewerbepathol. Gewerbehyg. 19, 613–632.
Holdenrieder, S., Stieber, P., 2010. Circulating apoptotic markers in the management of non-small cell lung cancer. Cancer Biomark. 6, 197–210.
Holder, A.L., Goth-Goldstein, R., Lucas, D., Koshland, C.P., 2012. Particle-induced artifacts in the MTT and LDH viability assays. Chem. Res. Toxicol. 25, 1885–1892.

Huaux, F., Lasfargues, G., Lauwerys, R., Lison, D., 1995. Lung toxicity of hard metal particles and production of interleukin-1, tumor necrosis factor-alpha, fibronectin, and cystatin-c by lung phagocytes. Toxicol. Appl. Pharmacol. 132, 53–62.
Joseph, M., 1968. Hard metal pneumoconiosis. Australas. Radiol. 12, 92–95.
Kerfoot, E.J., Fredrick, W.G., Domeier, E., 1975. Cobalt metal inhalation studies on miniature swine. Am. Ind. Hyg. Assoc. J. 36, 17–25.
Kitamura, H., Yoshimura, Y., Tozawa, T., Koshi, K., 1980. Effects of cemented tungsten carbide dust on rat lungs following intratracheal injection of saline suspension. Acta Pathol. Jpn. 30, 241–253.
Kraus, T., Schramel, P., Schaller, K.H., Zobelein, P., Weber, A., Angerer, J., 2001. Exposure assessment in the hard metal manufacturing industry with special regard to tungsten and its compounds. Occup. Environ. Med. 58, 631–634.
Kroll, A., Pillukat, M.H., Hahn, D., Schnekenburger, J., 2012. Interference of engineered nanoparticles with in vitro toxicity assays. Arch. Toxicol. 86, 1123–1136.
Kuhnel, D., Busch, W., Meissner, T., Springer, A., Potthoff, A., Richter, V., Gelinsky, M., Scholz, S., Schirmer, K., 2009. Agglomeration of tungsten carbide nanoparticles in exposure medium does not prevent uptake and toxicity toward a rainbow trout gill cell line. Aquat. Toxicol. 93, 91–99.
Kuhnel, D., Scheffler, K., Wellner, P., Meissner, T., Potthoff, A., Busch, W., Springer, A., Schirmer, K., 2012. Comparative evaluation of particle properties, formation of reactive oxygen species and genotoxic potential of tungsten carbide based nanoparticles in vitro. J. Hazard. Mater. 227–228, 418–426.
Kusaka, Y., Kuwabara, O., Kitamura, H., 1984. A case of diffuse lung disease associated with lung cancer in a hard metal worker. Nihon Kyobu Shikkan Gakkai Zasshi 22, 804–808.
Lasfargues, G., Lison, D., Maldague, P., Lauwerys, R., 1992. Comparative study of the acute lung toxicity of pure cobalt powder and cobalt-tungsten carbide mixture in rat. Toxicol. Appl. Pharmacol. 112, 41–50.
Lasfargues, G., Wild, P., Moulin, J.J., Hammon, B., Rosmorduc, B., Rondeau du Noyer, C., Lavandier, M., Moline, J., 1994. Lung cancer mortality in a French cohort of hard-metal workers. Am. J. Ind. Med. 26, 585–595.
Lasfargues, G., Lardot, C., Delos, M., Lauwerys, R., Lison, D., 1995. The delayed lung responses to single and repeated intratracheal administration of pure cobalt and hard metal powder in the rat. Environ. Res. 69, 108–121.
Li, J., S, M., Ng, C., LY, Y., BH, B., 2010. Nanoparticle-induced pulmonary toxicity. Exp. Biol. Med. 235, 1025–1033.
Lison, D., Lauwerys, R., 1990. In vitro cytotoxic effects of cobalt-containing dusts on mouse peritoneal and rat alveolar macrophages. Environ. Res. 52, 187–198.
Lison, D., Lauwerys, R., 1992. Study of the mechanism responsible for the elective toxicity of tungsten carbide-cobalt powder toward macrophages. Toxicol. Lett. 60, 203–210.
Lison, D., Lauwerys, R., 1993. Evaluation of the role of reactive oxygen species in the interactive toxicity of carbide-cobalt mixtures on macrophages in culture. Arch. Toxicol. 67, 347–351.
Lison, D., Carbonnelle, P., Mollo, L., Lauwerys, R., Fubini, B., 1995. Physicochemical mechanism of the interaction between cobalt metal and carbide particles to generate toxic activated oxygen species. Chem. Res. Toxicol. 8, 600–606.
Lombaert, N., De Boeck, M., Decordier, I., Cundari, E., Lison, D., Kirsch-Volders, M., 2004. Evaluation of the apoptogenic potential of hard metal dust (WC-Co), tungsten carbide and metallic cobalt. Toxicol. Lett. 154, 23–34.
Lombaert, N., Lison, D., Van Hummelen, P., Kirsch-Volders, M., 2008. In vitro expression of hard metal dust (WC-Co)–responsive genes in human peripheral blood mononucleated cells. Toxicol. Appl. Pharmacol. 227, 299–312.
Lombaert, N., Castrucci, E., Decordier, I., Van Hummelen, P., Kirsch-Volders, M., Cundari, E., Lison, D., 2012. Hard-metal (WC-Co) particles trigger a signaling cascade involving p38 MAPK, HIF-1alpha, HMOX1, and p53 activation in human PBMC. Arch. Toxicol. 87, 259–268.
Luo, H., Jiang, B., Li, B., Li, Z., Jiang, B.H., Chen, Y.C., 2012. Kaempferol nanoparticles achieve strong and selective inhibition of ovarian cancer cell viability. Int. J. Nanomedicine 7, 3951–3959.
Mariano, A., Sartorelli, P., Innocenti, A., 1994. Evolution of hard metal pulmonary fibrosis in two artisan grinders of woodworking tools. Sci. Total Environ. 150, 219–221.
Matejka, M.H., Wernisch, J., Lill, W., Fuchsjager, E., Watzek, G., 1985. Heavy metal deposits in pathologically modified hard tissues. Clinical and experimental studies. Wien. Med. Wochenschr. 135, 523–525.
Migliori, M., Mosconi, G., Michetti, G., Belotti, L., D'Adda, F., Leghissa, P., Musitelli, O., Cassina, G., Motta, T., Seghizzi, P., et al., 1994. Hard metal disease: eight workers with interstitial lung fibrosis due to cobalt exposure. Sci. Total Environ. 150, 187–196.
Moriyama, H., Kobayashi, M., Takada, T., Shimizu, T., Terada, M., Narita, J., Maruyama, M., Watanabe, K., Suzuki, E., Gejyo, F., 2007. Two-dimensional analysis of elements and mononuclear cells in hard metal lung disease. Am. J. Respir. Crit. Care Med. 176, 70–77.
Moulin, J.J., Wild, P., Romazini, S., Lasfargues, G., Peltier, A., Bozec, C., Deguerry, P., Pellet, F., Perdrix, A., 1998. Lung cancer risk in hard-metal workers. Am. J. Epidemiol. 148, 241–248.
Naqvi, A.H., Hunt, A., Burnett, B.R., Abraham, J.L., 2008. Pathologic spectrum and lung dust burden in giant cell interstitial pneumonia (hard metal disease/cobalt pneumonitis): review of 100 cases. Arch. Environ. Occup. Health 63, 51–70.
Nemery, B., Abraham, J.L., 2007. Hard metal lung disease: still hard to understand. Am. J. Respir. Crit. Care Med. 176, 2–3.
Nemery, B., Verbeken, E.K., Demedts, M., 2001. Giant cell interstitial pneumonia (hard metal lung disease, cobalt lung). Semin. Respir. Crit. Care Med. 22, 435–448.
Nunez, J., Fellous, A., Francon, J., Lennon, A.M., 1979. Competitive inhibition of colchicine binding to tubulin by microtubule-associated proteins. Proc. Natl. Acad. Sci. U. S. A. 76, 86–90.
Nurkiewicz, T.R., Porter, D.W., Hubbs, A.F., Stone, S., Moseley, A.M., Cumpston, J.L., Goodwill, A.G., Frisbee, S.J., Perrotta, P.L., Brock, R.W., Frisbee, J.C., Boegehold, M.A., Frazer, D.G., Chen, B.T., Castranova, V., 2011. Pulmonary particulate matter and systemic microvascular dysfunction. Res. Rep. Health Eff. Inst. 3–48.
Park, E.J., Yi, J., Chung, K.H., Ryu, D.Y., Choi, J., Park, K., 2008. Oxidative stress and apoptosis induced by titanium dioxide nanoparticles in cultured BEAS-2B cells. Toxicol. Lett. 180, 222–229.
Rengasamy, A., Kommineni, C., Jones, J.A., Fedan, J.S., 1999. Effects of hard metal on nitric oxide pathways and airway reactivity to methacholine in rat lungs. Toxicol. Appl. Pharmacol. 157, 178–191.
Rivolta, G., Nicoli, E., Ferretti, G., Tomasini, M., 1994. Hard metal lung disorders: analysis of a group of exposed workers. Sci. Total Environ. 150, 161–165.
Rizzato, G., Fraioli, P., Sabbioni, E., Pietra, R., Barberis, M., 1992. Multi-element follow up in biological specimens of hard metal pneumoconiosis. Sarcoidosis 9, 104–117.
Roesems, G., Hoet, P.H., Dinsdale, D., Demedts, M., Nemery, B., 2000. In vitro cytotoxicity of various forms of cobalt for rat alveolar macrophages and type II pneumocytes. Toxicol. Appl. Pharmacol. 162, 2–9.
Ruokonen, E.L., Linnainmaa, M., Seuri, M., Juhakoski, P., Soderstrom, K.O., 1996. A fatal case of hard-metal disease. Scand. J. Work Environ. Health 22, 62–65.
Schutze, S., Machleidt, T., Adam, D., Schwandner, R., Wiegmann, K., Kruse, M.L., Heinrich, M., Wickel, M., Kronke, M., 1999. Inhibition of receptor internalization by monodansylcadaverine selectively blocks p55 tumor necrosis factor receptor death domain signaling. J. Biol. Chem. 274, 10203–10212.
Shivapurkar, N., Reddy, J., Chaudhary, P.M., Gazdar, A.F., 2003. Apoptosis and lung cancer: a review. J. Cell. Biochem. 88, 885–898.
Simeonova, P.P., Erdely, A., 2009. Engineered nanoparticle respiratory exposure and potential risks for cardiovascular toxicity: predictive tests and biomarkers. Inhal. Toxicol. 21 (Suppl. 1), 68–73.
Song, Y., Li, X., Du, X., 2009. Exposure to nanoparticles is related to pleural effusion, pulmonary fibrosis and granuloma. Eur. Respir. J. 34, 559–567.
Stearns, R.C., Paulauskis, J.D., Godleski, J.J., 2001. Endocytosis of ultrafine particles by A549 cells. Am. J. Respir. Cell Mol. Biol. 24, 108–115.
Stefaniak, A.B.., Day, G.A., Harvey, C.J., Leonard, S.S., Schwegler-Berry, D.E., Chipera, S.J., Sahakian, N.M., Chisholm, W.P., 2007. Characteristics of dusts encountered during the production of cemented tungsten carbides. Ind. Health 45, 793–803.
Stefaniak, A.B.., Virji, M.A., Day, G.A., 2009. Characterization of exposures among cemented tungsten carbide workers. Part I: Size-fractionated exposures to airborne cobalt and tungsten particles. J. Expo. Sci. Environ. Epidemiol. 19, 475–491.
Stieber, P., Holdenrieder, S., 2010. Lung cancer biomarkers - Where we are and what we need. Cancer Biomark. 6, 221–224.
Sun, L., Li, Y., Liu, X., Jin, M., Zhang, L., Du, Z., Guo, C., Huang, P., Sun, Z., 2011. Cytotoxicity and mitochondrial damage caused by silica nanoparticles. Toxicol. In Vitro 25, 1619–1629.
Trautmann, H., 1958. Pneumoconiosis due to inhaltion of hard metal dusts. Hefte Unfallheilkd. 56, 99–103.
Val, S., Hussain, S., Boland, S., Hamel, R., Baeza-Squiban, A., Marano, F., 2009. Carbon black and titanium dioxide nanoparticles induce pro-inflammatory responses in bronchial epithelial cells: need for multiparametric evaluation due to adsorption artifacts. Inhal. Toxicol. 21 (Suppl. 1), 115–122.
Wang, X.F., Ding, B., Li, B.Y., 2013. Biomimetic electrospun nanofibrous structures for tissue engineering. Mater. Today 16, 229–241.
Wilhelmi, V., Fischer, U., van Berlo, D., Schulze-Osthoff, K., Schins, R.P., Albrecht, C., 2012. Evaluation of apoptosis induced by nanoparticles and fine particles in RAW 264.7 macrophages: facts and artefacts. Toxicol. In Vitro 26, 323–334.
Wu, Y.-L., Putcha, N., Ng, K.W., Tai Leong, D., Lim, C.T., Loo, S.C.J., Chen, X., 2012. Biophysical Responses upon the Interaction of Nanomaterials with Cellular Interfaces. Acc. Chem. Res. 46, 782–791.
Yao, Z., Stiglich, J., Sudarshan, T., 1998. Nanosized WC-Co holds promise for the future. Metal Powder Rep. 53, 26–33.
Zhang, L.W., Monteiro-Riviere, N.A., 2009. Mechanisms of quantum dot nanoparticle cellular uptake. Toxicol. Sci. 110, 138–155.
Zhang, X.D., Zhao, J., Bowman, L., Shi, X., Castranova, V., Ding, M., 2010. Tungsten carbide-cobalt particles activate Nrf2 and its downstream target genes in JB6 cells possibly by ROS generation. J. Environ. Pathol. Toxicol. Oncol. 29, 31–40.
Zhao, J., Castranova, V., 2011. Toxicology of nanomaterials used in nanomedicine. J. Toxicol. Environ. Health B Crit. Rev. 14, 593–632.